Thermal Broadening Analysis of the Light Harvesting Complex II Absorption Spectrum

Giuseppe Zucchelli,* Flavio M. Garlaschi, and Robert C. Jennings

Centro CNR Biologia Cellulare e Molecolare Piante, Dipartimento di Biologia, Università di Milano, Via Celoria 26, 20133 Milano, Italy

Received June 4, 1996; Revised Manuscript Received September 18, 1996[⊗]

ABSTRACT: Absorption spectra in the Q_y region of the light harvesting complex II (LHCII) have been measured in the temperature range 70−300 K. The spectra were analyzed by evaluating the temperature dependence (a) of the total bandwidth and (b) of the sub-bands obtained by numerical decomposition in terms of double Gaussians. The thermal broadening of the bands are interpreted, in both cases, as a homogeneous component, due to the presence of linear electron−phonon coupling, plus an inhomogeneous component, due to both statistical energy fluctuations at each pigment site and heterogeneity of the sample itself. Sub-bands analysis, in which eight major components are identified, yields a reorganization energy $9\ cm^{-1} \leq S\nu_m \leq 14\ cm^{-1}$ and an inhomogeneous contribution in the range 120−170 cm^{-1}. In all cases the bands are substantially symmetrical in the 70−300 K temperature range. This observation gains theoretical support from an analysis of the band moments, when the influence of a low-frequency vibrational mode is considered. Analysis of the total absorption band yields $S\nu_m \approx 70\ cm^{-1}$; however, this high value is reduced to $S\nu_m \approx 11-20\ cm^{-1}$ when the red-most sub-band, with maximum at 684 nm, is eliminated at all temperatures. These data are discussed in terms of the underlying transitions, giving strong support to the presence of extreme red absorption bands in LHCII. The presence of another low-frequency mode with $\nu_m > 20-30\ cm^{-1}$ is also proposed.

In higher plants, chromophores, mainly chl[1] *a* and chl *b* molecules, are organized in large arrays which absorb light. The resulting electronic excitation is transferred to the reaction centers where photochemical trapping occurs. PSII antenna contains about 200−250 chl molecules per reaction center and consists of at least six different chl−protein complexes (for a review see Jennings et al., 1996). Two of these, CP43 and CP47, contain only chl *a* and are closely associated with the RC. The other four complexes contain both chl *a* and chl *b* in different ratios (Dainese & Bassi, 1991) and are identified as the external antenna. One of these, the major light harvesting antenna complex, is the chl *a*/*b* protein complex LHCII. It binds about 50% of the total chlorophyll and is the most abundant membrane protein in plants. Crystallography of this complex at 6 Å (Kühlbrandt & Wang, 1991) and 3.4 Å (Kühlbrandt et al., 1994) resolution indicates a trimeric basic unit of symmetrically arranged monomers containing about 12 chl molecules each (7 chl *a* and 5 chl *b*). The chlorophyll molecules seem to be arranged on two levels with an estimated nearest-neighbor distance between centers of chls on the same level in the range 9−14 Å (Kühlbrandt et al., 1994), a distance very similar to the chl tetrapyrrole ring diameter (∼8 Å, Kühlbrandt et al., 1994). This closely packed organization suggests the possibility of excitonic interactions between chromophores but, to date, clear direct evidence for their presence is lacking. For chl *b* Gülen and Knox (1984) have proposed, extending an earlier analysis (van Metter, 1977), an arrangement with C_3 symmetry, giving rise to exciton splitting with transitions at about 666 nm (nondegenerate) and 653 nm (2-fold degenerate). However, from LHCII crystallography (Kühlbrandt & Wang, 1991; Kühlbrandt et al., 1994), the presence of a C_3 symmetry between the identified chromophores seems to be absent, though the trimeric complex has a C_3 symmetry and an interaction between chl *b* molecules on different monomers cannot be excluded. The presence of excitonic interactions chl *b*−chl *b*, chl *b*−chl *a*, and also chl *a*−chl *a* has been suggested (Ide et al., 1987; Hemelrijk et al., 1992) by low temperature analysis of LHCII optical spectra.

The very complicated spectroscopic properties of LHCII have been analyzed using different techniques both at cryogenic temperatures and at RT (Zucchelli et al., 1990, 1992; Kwa et al., 1992; Hemelrijk et al., 1992; Krawczyk et al., 1993; Reddy et al., 1994; Nussberger et al., 1994). Considerable spectral congestion, with at least 5−7 separate transitions in the wavelength range 660−684 nm, plus contributions due to chl *b* in the wavelength range around and below 650 nm is suggested. The presence of these different transitions is quite intriguing as chl *a* in different solvents exibits a maximum absorption around 661−665 nm (Seely & Jensen, 1965; Porra, 1991). A possible explanation, first proposed by French and co-workers (1972), is that chl molecules in different protein environments change their spectral characteristics, thus giving rise to different spectral forms. The possibility of modulation of the light absorption properties of porphyrins has been recently supported by calculations on the consequences of conformational distortions of the porphyrin skeleton imposed by the host protein (Gudowska-Nowak et al., 1990). The number of separate transitions proposed to describe the absorption spectrum of

[⊗] Abstract published in *Advance ACS Abstracts,* November 1, 1996.

[1] Abbreviations: chl, chlorophyll; CP, chlorophyll protein complex; FWHM, full width at half-maximum; $FWHM_{hom}$, homogeneous part of the width; $FWHM_{inh}$, inhomogeneous part of the width; LHCII, light harvesting complex II; PSII, photosystem II; RT, room temperature; σ, root mean square deviation from the mean.

S0006-2960(96)01317-7 CCC: $12.00

LHCII is always less than the number of chl molecules in the LHCII monomer. This can be due to the presence of more than one chlorophyll in protein environments which generate very similar absorption properties, but the presence of unresolved transitions cannot be excluded with certainty. In addition to the presence of different spectral forms, it seems probable that the band shapes may be modified by the protein host environment with respect to that of chl in vitro. Hole burning studies (Gillie et al., 1989; Reddy et al., 1994) have indicated the presence of 20−30 cm^{-1} nuclear vibrational modes in chl−protein complexes to which pigment electronic transitions are coupled. These vibrational coupling modes, presumably absent in organic solvents, are expected to have a significant role in determining the width of chlorophyll absorption bands in chl−protein complexes. Furthermore, these vibrational coupling parameters will also influence band symmetry (Lax, 1952).

An important problem is the characterization of these buried transitions constituting the chl−protein complex absorption spectrum, as these properties are of fundamental importance in understanding energy transfer within the chromophore array. Direct experimental evidence of sub-band characteristics are limited to the red-most wavelength region of the LHCII absorption, where the reorganization energy and the inhomogeneous contribution to the total bandwidth have been obtained by the hole burning technique at 4 K (Reddy et al., 1994). Moreover, the action spectrum for hole burning in the red part of the LHCII absorption gives a profile that can be described by a Gaussian band shape peaking at 680 nm with a FWHM ≈100 cm^{-1}. Furthermore, analysis of the red wing of the 680 nm hole indicates the presence of a transition band around 684 nm. At RT a sub-band peaking at 684 nm, that decreases its contribution upon lowering the temperature, has been proposed (Zucchelli et al., 1990, 1994) using numerical decomposition techniques.

A weak coupling ($S < 1$) of the electronic transition to a distribution of low-frequency phonon modes, having a mean frequency around 20−30 cm^{-1}, seems to be responsible for the homogeneous band broadening of the transitions associated with chls in a host protein matrix (Gillie et al., 1989; Reddy et al., 1994). From the reorganization energy and $FWHM_{inh}$, the temperature broadening evolution of an absorption band can be calculated (Lax, 1952; Dexter, 1958; Markham, 1959; Chan & Page, 1983; Schomacker & Champion, 1986; Hayes et al., 1988; Di Pace et al., 1992). We report here a temperature analysis, in the range 70−300 K, of the $Q_y(0,0)$ region of the LHCII absorption spectrum, where only chls absorb, both of the entire band and using numerical sub-band decomposition. The decomposition approach to thermal broadening has already been used to analyze the D1/D2/cytb559 absorption spectrum (Cattaneo et al., 1995). In this way it has been possible to assign both reorganization energy and inhomogeneous broadening contributions to the main chl *a* sub-bands. The values obtained are in agreement with the limited data obtained by hole burning at 4 K for LHCII and suggest that the band shape is substantially symmetrical for T ≥ 70 K.

MATERIALS AND METHODS

LHCII was prepared essentially as described by Ryrie et al. (1980).

Absorption spectra of the complex were measured using an OMAIII (EG&G, Model 1460) with an intensified diode array detector (Model 1420) mounted on a spectrograph (Jobin-Yvon, Model HR320) with a 150 nm mm^{-1} grating. The wavelength spacing between pixels is below 0.5 nm in this configuration. The wavelength scale of the instrument was calibrated using a spectral line calibration source (Cathodeon). The light source was a halogen lamp attenuated by neutral filters (Balzers) and filtered through an LP560 (Balzers) to eliminate the blue part of the incident radiation. The light path was 1 mm, and sample absorption was measured in the temperature range 70−300 K using a vacuum-assisted Joule-Thomson refrigerating system (Model K-2002T, MMR Tech.). Samples were diluted in a buffer containing Tricine, 50 mM (pH 8); glycerol, 80% (v/v); octyl glucoside, 0.4%. Each spectrum is the result of summing 10^4 scans to achieve a good signal to noise ratio. The residual absorption at wavelengths greater than 720 nm were subtracted from the spectra, when present.

Numerical decomposition of the absorption spectra, at all temperatures measured, has been performed as previously described (Jennings et al., 1993; Zucchelli et al., 1994), using an algorithm that minimizes the χ^2 function with respect to the parameters of a model function defined as a linear combination of Gaussian functions. Each Gaussian is defined as the sum of two half Gaussians (double Gaussian). In this way each sub-band has two independent bandwidths, right and left, and this can, in principle, describe the presence of asymmetry (see Discussion).

All photosynthetic complexes seem to be characterized by great spectral congestion that greatly complicates analysis. From the numerical point of view, the minimization problem over the χ^2 hyperspace is formidable, due to the presence of secondary minima that can bias the reaching of the global minimum. The goodness of the minimum attained was judged by using the reduced χ^2 values, the distribution of the errors (Bevington & Robinson, 1992; Eadie et al., 1971), and comparison between the second derivative of the measured and calculated spectra. All the fits obtained differ with respect to the measured spectra by less than 0.01% along the fitted interval.

The thermal broadening of an absorption spectrum due to coupling of the electronic transition with a bath of phonon modes, characterized by a mean frequency ν_m and coupling strength S, can be described using σ^2, the root mean square deviation from the mean of the absorption distribution (Lax, 1952; Stepanov & Gribkovskii, 1968; Eadie et al., 1971). For a Gaussian function it is possible to express σ^2 in terms of the spectroscopically more usual FWHM:

$$FWHM_{hom}^{\ 2} = (8 \ln 2) S \nu_m^{\ 2} \coth\left(\frac{hc\nu_m}{2k_B T}\right) \qquad (1)$$

where c is the light velocity, h is the Planck constant, k_B is the Boltzmann constant, and T is the temperature; ν_m and FWHM are in cm^{-1} units. This equation has been widely used to describe the homogeneous broadening contribution to the chl absorption in a host protein complex (see, e.g., Hayes et al., 1988). When $h\nu_m c < 2k_B T$, $\coth(h\nu_m c/2k_B T) \approx (2k_B T/h\nu_m c)$, and eq 1 simplifies to:

$$FWHM_{hom}^{\ 2} \approx 7.7 S \nu_m T \qquad (2)$$

a straight line with respect to temperature.

Table 1: Decomposition Sub-Band Parameters of the LHCII Absorption Spectra[a]

	71 K	100 K	130 K	170 K	210 K	250 K	270 K	296 K
λ_{max} (nm)	643.8	643.8	643.7	643.8	643.9	643.9	644.0	644.0
FWHM (cm^{-1})	196.0	199.0	202.4	206.2 ± 0.6	219.9 ± 2.3	227.9 ± 1.2	226.7 ± 1.2	227.6 ± 1.3
area (%)	9.7	9.5	9.2	8.6	9.2 ± 1.5	8.4	8.0	8.3
λ_{max} (nm)	650.0	650.0	650.0	650.0	650.0	650.5	650.5	650.5
FWHM (cm^{-1})	191.4 ± 0.5	194.0	201.2	205.8	211.9 ± 0.5	218.6 ± 0.5	219.7 ± 1	217.3 ± 7
area (%)	18.6 ± 0.1	18.1	18.2	17.3 ± 0.1	15.6 ± 0.1	14.9 ± 0.2	14.5 ± 0.3	14.0 ± 0.3
λ_{max} (nm)	656.0	656.0	656.0	656.0	656.0	656.0	656.0	656.0
FWHM (cm^{-1})	182.2 ± 0.4	186.7 ± 0.2	194.4 ± 0.2	197.4 ± 0.6	201.4 ± 0.3	208.3 ± 0.7	216.0 ± 4.0	211.7 ± 2.1
area (%)	13.3	13.5	13.1	12.8 ± 0.1	12.3	12.1 ± 0.1	12.8 ± 1.0	11.7 ± 0.2
λ_{max} (nm)	661.5	661.5	661.5	661.5	661.5	661.5	661.5	661.5
FWHM (cm^{-1})	180.3 ± 1.8	181.6 ± 1.0	192.4 ± 1.0	198.9 ± 2.0	205.1 ± 1.0	211.7 ± 2.0	215.2 ± 3.5	218.0 ± 2.3
area (%)	15.0 ± 0.1	14.1 ± 0.1	13.1 ± 0.1	13.0 ± 0.2	12.5	12.3 ± 0.2	11.1 ± 1.0	11.95 ± 0.2
λ_{max} (nm)	667.0	666.5	666.5	666.5	666.5	666.5	666.5	666.5
FWHM (cm^{-1})	177.1 ± 6.0	175.8 ± 1.8	181.6 ± 1.5	183.6 ± 2.8	202.9 ± 5.4	205.3 ± 6.2	210.1 ± 7.1	210.8 ± 6.2
area (%)	16.1 ± 1.0	15.4 ± 0.5	14.4 ± 0.5	13.2 ± 1.0	14.4 ± 1.0	13.8 ± 1.0	13.6 ± 1.0	13.3 ± 1.0
λ_{max} (nm)	672.0	672.0	672.0	672.0	672.0	672.0	672.0	672.0
FWHM (cm^{-1})	152.8 ± 1.9	159.1 ± 1.1	167.7 ± 2.8	177.5 ± 3.2	196.1 ± 5.6	201.1 ± 3.1	205.6 ± 2.3	206.8 ± 4.4
area (%)	20.8 ± 1.7	21.2 ± 0.6	21.8 ± 0.7	20.6 ± 1.0	20.1 ± 1.7	20.1 ± 1.9	20.4 ± 1.4	19.8 ± 2.5
λ_{max} (nm)	677.5	677.5	678.0	678.0	678.5	678.5	678.5	678.5
FWHM (cm^{-1})	152.3 ± 4.9	162.5 ± 4.9	165.4 ± 2.8	182.1 ± 3.5	197.5 ± 2.8	210.9 ± 1.0	211.9 ± 2.9	213.9 ± 4
area (%)	28.6 ± 1.6	28.3 ± 1.2	27.9 ± 1.0	28.1 ± 1.0	25.8 ± 1.0	25.2 ± 1.0	25.1 ± 1.2	24.2 ± 1.0
λ_{max} (nm)	683.0	683.0	683.0	683.0	683.0	684.0	684.5	684.5
FWHM (cm^{-1})	142.2 ± 7.1	164.9 ± 3.2	178.4 ± 1.3	195.5 ± 3.0	212.8 ± 5.5	225.6 ± 6.0	228.0 ± 3.6	227.0 ± 3.3
area (%)	4.2 ± 1.4	6.1 ± 0.9	8.1 ± 0.5	10.1 ± 0.5	12.6 ± 0.6	13.4 ± 1.0	14.4 ± 0.8	15.8 ± 1.5

[a] The percentage absorption has been calculated, for each decomposition utilized to evaluate the mean values, with respect to the area of all the sub-bands starting from the 656 nm sub-band. The contribution due to the extreme red sub-band, $\lambda_{max} \approx 690$ nm, is not shown due to the uncertainty of its parameters' values.

In the presence of an inhomogeneous contribution, due, e.g., to statistical fluctuations of the chromophore environment or to sample inhomogeneity, the measured FWHM of an absorption band can be described by:

$$\mathrm{FWHM}^2 = \mathrm{FWHM}_{\mathrm{hom}}{}^2 + \mathrm{FWHM}_{\mathrm{inh}}{}^2 \qquad (3)$$

as the results of the convolution of the homogeneous Gaussian band with the inhomogeneous Gaussian distribution (see, e.g., Hayes et al., 1988).

These expressions, or the equivalent expressions written in terms of σ^2, have been used in the present study to analyze the temperature dependence of the LHCII absorption spectra in the temperature range 70−300 K as well as the temperature dependence of the sub-bands obtained by numerical decomposition. Information on the reorganization energy $S\nu_m$ and the inhomogeneous contribution associated with each sub-band is thus obtained.

RESULTS

The absorption spectra of LHCII were measured in the wavelength range 630−720 nm, at various temperatures between 70 and 300 K, and analyzed in terms of Gaussian sub-bands. The parameters of these sub-bands, obtained as a mean of different fits, are reported in Table 1. The percentage differences between measured and numerical spectra are below 0.01% (data not shown), along the fitted region, for all the spectra used to calculate the mean values. Figure 1 shows the spectra at the two extreme temperatures together with typical decompositions; the residuals plots are also shown.

The wavelength maximum of the absorption shifts slightly toward the blue side on lowering the temperature, as already observed (Zucchelli et al., 1994). The total area of the measured spectra remains constant in the temperature interval analyzed, and all the temperature-induced spectral changes are reversible (data not shown).

The Gaussian sub-band description reported here differs from our previous attempts (Zucchelli et al., 1992, 1994; Jennings et al., 1993) by the presence of two more sub-bands; one in the 655−662 nm wavelength region, the other in the region around 670 nm. In particular, the presence of more than one sub-band in the 655−662 nm region describes better the small but clear "structure" observed there at low temperature (Figure 1), that is also clearly seen in the second derivative shown in Figure 2. At RT, only three clear structures are resolved (∼651, 673, 681 nm), while other structures appear upon lowering the temperature (∼650, 657, 662, 671, 677 nm). Even though it is not clearly seen in Figures 1 and 2, addition of a further sub-band in the region around 670 nm was suggested by the CD and absorption spectra (77 K) reported by Nussberger et al. (1994). The greater number of sub-bands increases the already great numerical difficulties due to the cross correlations between parameters. In order to partly overcome this problem, the stability of each parameter minimum, i.e., the stability of a particular numerical description, has been checked by moving around the minimum in the parameters hyperspace. Different fits have been considered such that the percentage difference between calculated and measured spectra was always below 0.01%. These fits have been used to calculate the mean parameter values and the relative errors reported in Table 1. With this sub-band description, very small, high-frequency residual oscillations can be obtained as well as a total coincidence of the second derivative of measured and numerical spectra (data not shown).

The squared FWHM temperature dependence of the chl *a* sub-bands peaked at about 678, 672, 667, and 661 nm are shown in Figure 3. The linear fits of these data are also reported and the values obtained according to equation 2 and 3 are shown in Table 2. The reorganization energies obtained

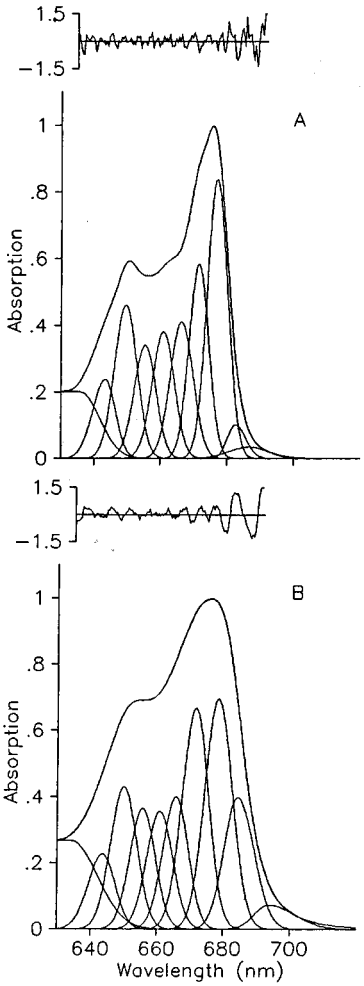

FIGURE 1: LHCII absorption spectra measured at 70 K (A) and 300 K (B). Gaussian sub-band decompositions are also shown with the residual plots calculated as the ratio measured spectrum minus the calculated spectrum with respect to the statistical errors of the measured spectrum. The percentage difference between measured and numerical spectra is below 0.01% along the fitted interval.

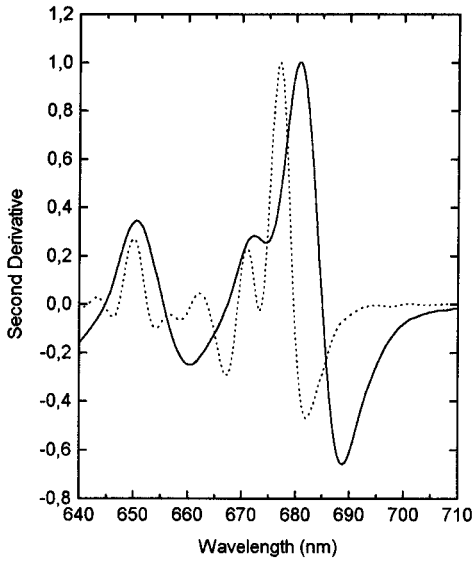

FIGURE 2: Second derivative of the LHCII absorption spectra measured at 70 and 300 K. The plots are multiplied by −1. (—) 300 K, (···) 70 K.

are in the interval 9 $cm^{-1} \leq S\nu_m \leq 14$ cm^{-1}, and the values are similar for all the major sub-bands. This means that, taking the mean phonon frequency $\nu_m \cong 20$ cm^{-1}, as indicated by hole burning experiments in different chl−protein complexes (Hayes et al., 1988; Gillie et al., 1989; Reddy et al., 1994), the interval for the linear coupling coefficient $0.45 \leq S \leq 0.70$ is estimated. These values are in fairly good agreement with those estimated from the limited hole burning data for chl *a* in LHCII at low temperature (Reddy et al., 1994). The inhomogeneous contribution to the total bandwidth of the sub-bands is in the range 120−170 cm^{-1} and increases on going toward the shorter wavelength sub-bands.

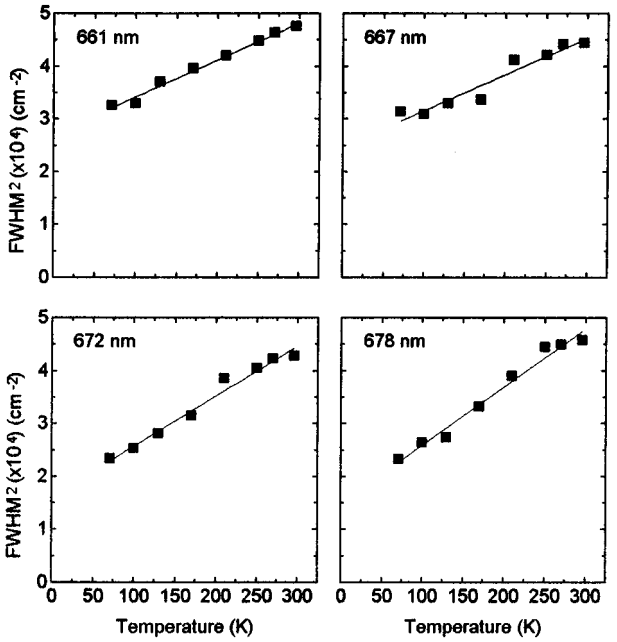

FIGURE 3: Plots of the squared FWHM of the main sub-bands constituting the LHCII absorption spectra with respect to temperature. Linear fits of the data are also shown and the corresponding parameters are reported in Table 2.

Table 2: Reorganization Energy and the Inhomogeneous Contribution of LHCII Sub-Bands

	λ_{max} (nm)			
	661.5	667.0	672.0	678.0
$S\nu_m$ (cm^{-1})	9.1 ± 0.4	8.9 ± 1.0	12.3 ± 0.7	14.3 ± 0.8
$FWHM_{inh}$ (cm^{-1})	165 ± 2	157 ± 5	128 ± 4	122 ± 5

This sub-band analysis confirms our previous suggestions concerning the presence of a sub-band, with significant intensity at higher temperatures, at 684 nm (Zucchelli et al., 1990, 1992, 1994). From Figure 4 it is clear that the intensity of this band changes continuously with sample temperature, decreasing in an apparently linear fashion upon lowering the temperature. This process is reversible (data not shown).

We wish to point out that, though the decomposition program used in the present study allows for band asymmetry, all sub-bands come out substantially symmetrical, in agreement with earlier studies (Zucchelli et al., 1990, 1992, 1994). This important point is further developed in the Discussion.

In Figure 5, data are presented for the thermal broadening of the entire absorption spectrum and after subtraction of the sub-bands up to and including that at 650 nm. It is demonstrated in the Appendix that the temperature-induced changes of the total bandwidth of the absorption spectrum can be directly connected to the temperature-induced changes

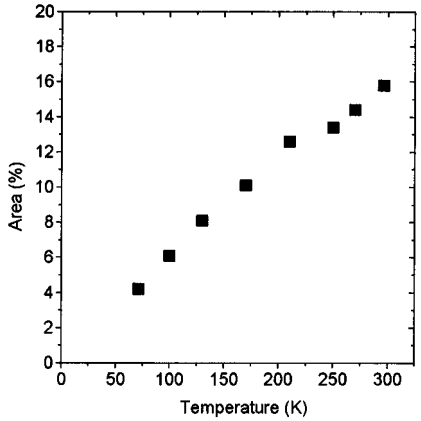

FIGURE 4: Area contribution of the 684 nm sub-band to the $Q_y(0,0)$ LHCII absorption. The data are taken from Table 1.

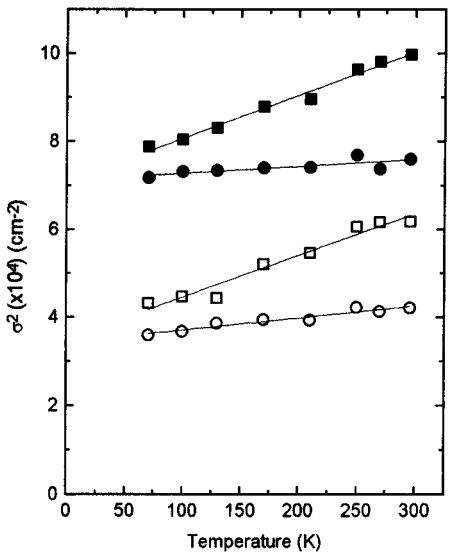

FIGURE 5: The second order central moment, σ^2, of the LHCII $Q_y(0,0)$ absorption band with respect to temperature. (■) σ^2 calculated for the entire absorption band starting at 15 600 cm^{-1} (~640 nm); (●) as before but after subtraction of the sub-bands peaking in the long wavelength region $\lambda \geq 683$ nm. The linear fit (also shown) gives (■) $S\nu_m \approx 70$ cm^{-1}, $\sigma_{inh} \approx 266$ cm^{-1}; (●) $S\nu_m \approx 11$ cm^{-1}, $\sigma_{inh} \approx 266$ cm^{-1}. (□) σ^2 calculated after subtraction of the short wavelength sub-bands up to the 650 nm sub-band; (○) as before but after subtraction of the sub-bands peaking in the long wavelength region $\lambda \geq 683$ nm. The linear fit (also shown) gives (□) $S\nu_m \approx 70$ cm^{-1}, $\sigma_{inh} \approx 187$ cm^{-1}; (○) $S\nu_m \approx 20$ cm^{-1}, $\sigma_{inh} \approx 185$ cm^{-1}.

of the underlying transitions (eq A.5). We have therefore calculated the σ^2 values for the LHCII absorption spectrum at different temperatures, which are seen to increase linearly with temperature. Analyzing this temperature dependence in terms of eq A.6, a "reorganization energy" $S\nu_m \cong 70$ cm^{-1} and an "inhomogeneous width" $\sigma_{inh} \cong 266$ cm^{-1} are obtained for the entire absorption band whereas $S\nu_m \cong 70$ cm^{-1} and $\sigma_{inh} \cong 187$ cm^{-1} are obtained without the sub-bands up to and including that at 650 nm. If the chl pigments responsible for the $Q_y(0,0)$ LHCII absorption have a similar coupling to a mean phonon frequency and the distribution of the different chl forms is independent of temperature, the $S\nu_m$ value obtained analyzing the total spectrum should be that of the chl forms (eq A.6). Chlorophylls in different chl−protein complexes have reorganization energies in the range 8 $cm^{-1} \leq S\nu_m \leq 16$ cm^{-1}, as obtained by hole burning, well below the value obtained by analysis of the entire LHCII absorption band. On the other hand, if σ^2 values are calculated from the absorption spectra as above but after subtraction of the sub-bands peaking at around 684 nm and at longer wavelengths (Figure 5), a linear temperature dependence is mantained but with a much smaller angular coefficient. A "reorganization energy" $S\nu_m \cong 11-20$ cm^{-1} and an "inhomogeneous contribution" $\sigma_{inh} \cong 185-266$ cm^{-1} are obtained. Despite the considerable errors present in these calculations, it can be seen that the "reorganization energy" thus obtained is similar to that obtained by hole burning. We wish to point out that "inhomogeneous contribution" is used in a general sense as it contains, in this case, both the statistical contributions as well as the term due to the presence of different underlying transitions.

DISCUSSION

In the present paper, the absorption spectra of the LHCII chl−protein complex, measured between 70 K $\leq T \leq$ 300 K and in the wavelength range 630−720 nm, have been analyzed in terms of a linear combination of Gaussian bands. Six main sub-bands are used to describe the wavelength range 650 nm $< \lambda \leq$ 700 nm. Two sub-bands in the wavelength region 655−662 nm yield a good description of the absorption and second derivative structures present (Figures 1 and 2) at low temperature. These absorption and second derivative structures almost completely disappear at room temperature. Thus a unique band peaking at around 660 nm is sufficient, at RT, to yield a good numerical fit, as found in previous attempts (Jennings et al., 1993; Zucchelli et al., 1994). The presence of these two sub-bands has been imposed for all the different temperatures. In the 670 nm region two sub-bands, peaking at 667 and 672 nm, are present. The inclusion of more than one sub-band in this wavelength region was suggested by CD and absorption spectroscopy of LHCII at low temperature (Nussberger et al., 1994). The main sub-band maximum is around 678 nm, with the significant red-most band peaking at around 684 nm. Two main sub-bands around 650 and 643 nm describe the blue part of the absorption spectra and are presumably mainly associated with chl *b*. This description, used at all the temperatures analyzed, yields calculated spectra that differ by less than 0.01% along the fitted region with respect to the measured spectra.

The spectral properties of these sub-bands depend essentially on the following: (a) coupling of the electronic transition to vibrational modes active in the chl−protein complex. A significant influence due to intramolecular vibrational modes is considered unlikely as the lowest frequency mode detected for chl *a* in a host protein matrix is around 262 cm^{-1}, with a very low coupling (0.012) (Gillie et al., 1989). (b) A contribution due to the inhomogeneity of the sample itself (heterogeneity) or associated with statistical fluctuations at the chromophore binding site, which can lead to a statistical modulation of the transition energy. These contributions can be described, in the approximation considered, by eq 3, and then, both reorganization energy $S\nu_m$ and the inhomogeneous broadening contribution, $FWHM_{inh}$, can be obtained for each sub-band. The reorganization energy values determined by linear fits of the squared FWHM (Figure 3) are similar for all the sub-bands analyzed and are in the range 9 $cm^{-1} \leq S\nu_m \leq 14$ cm^{-1} (Table 2). These $S\nu_m$ values are in reasonable agreement with the limited hole burning data for LHCII at 4 K (Reddy

et al., 1994) and are similar to the values obtained for chl *a* in other chl−protein complexes by the same technique (Gillie et al., 1989) as well as by the analysis of the temperature dependent properties of sub-bands recently performed for the D1/D2/cytb559 complex absorption spectrum (Cattaneo et al., 1995). All these data seem to indicate that chl *a* in different host protein matrices undergoes interactions with mean phonon active modes giving rise to a similar reorganization energy, and thus leading to similar spectral properties.

The $FWHM_{inh}$ seems to increase going toward the blue side of the spectrum and is in the range $120\ cm^{-1} \leq FWHM_{inh} \leq 170\ cm^{-1}$ (Table 2). This may indicate an increasing contribution of vibrational bands associated with the red-most spectral forms. However, the presence of unresolved transitions cannot be excluded. Available evidence suggests that the physical basis for the inhomogeneous broadening encountered in these LHCII samples is connected to statistical fluctuations associated with the pigment site energies rather than sample heterogeneity. In this context, it has been demonstrated that the Stepanov relation (Stepanov, 1957), which connects absorption and fluorescence spectra in the case of thermal equilibration of excited states, works well for LHCII at RT (Zucchelli et al., 1992). If the sample is heterogeneous, this is not the case (van Metter & Knox, 1976). Thus excitation seems to relax rapidly over the sample inhomogeneity during the excited state lifetime, a situation which is difficult to envisage in the case of significant sample heterogeneity.

An important problem concerning the characteristics of chlorophyll absorption bands in a host protein matrix is the band symmetry. The exact quantum mechanical treatment of the thermal broadening of the absorption lines for an electronic transition linearly coupled to vibrational normal modes has been performed by Lax (1952), yielding also the temperature dependence of the moments of the absorption band [see, e.g., Stepanov and Gribkovskii (1968) and Eadie et al., (1971) for the definition of moments]. This information, in principle, allows a complete description of an absorption band. In particular, the coefficient of skewness (Lax, 1952; Eadie et al., 1971), γ_1, which is directly related to the band symmetry, is given by:

$$\gamma_1 \equiv \frac{\bar{m}_3}{\sigma^3} = \frac{S\nu_m{}^3}{\left(S\nu_m{}^2 \coth\frac{h\nu_m}{2k_BT}\right)^{3/2}} = \frac{1}{\left(S\left(\coth\frac{h\nu_m}{2k_BT}\right)^3\right)^{1/2}} \quad (4)$$

where $\bar{m}_3$ is the central third order moment. γ_1 is zero for a symmetrical distribution. As can be seen from eq 4, the skewness coefficient is temperature dependent, reaching its maximum value for $T = 0$ and then decreasing for increasing temperatures. It also depends on the coupling factor S and the mean phonon frequency ν_m.

In the presence of weak coupling ($S < 1$) to a mean frequency of around $20-30\ cm^{-1}$, as suggested by hole burning studies for chls in a host protein matrix, the skewness coefficient is in the range 0.23−0.1 for $T = 70$ K and 1 order of magnitude less for $T = 300$ K (eq 4). This parameter is very general but difficult to envisage. However, owing to its importance in representing band symmetry, we have related it to the spectroscopically familiar FWHM, for a double Gaussian distribution, as a function of temperature. Data are presented in Figure 6 as the ratio of high and low energy side FWHM with respect to temperature. A FWHM ratio in the range 1.14−1.34 is estimated for the homogeneous broadening contribution to the linewidth at 70 K using couplings and mean frequencies in the range suggested by hole burning measurements. These values decrease to 1.01−1.03 at RT.

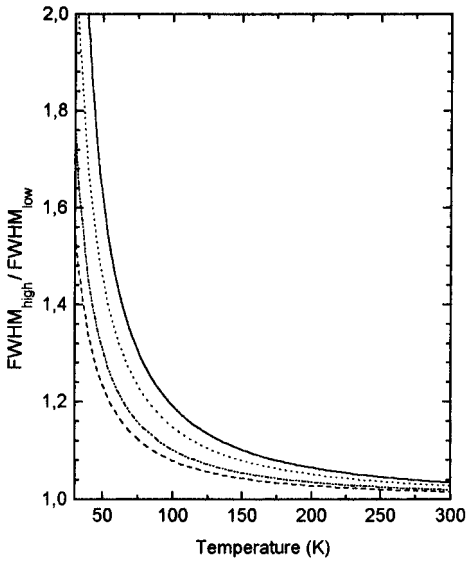

FIGURE 6: Plot of the ratio between the two FWHM of a double Gaussian with respect to temperature. The ratio is given as the width of the high energy side ($FWHM_{high}$) with respect to that of the low energy side ($FWHM_{low}$). The function is obtained comparing the expression of the skewness parameter γ_1 obtained for a double Gaussian with the theoretically predicted γ_1 temperature dependence (eq 4) for a homogeneous broadened band. (—) $S = 0.5$, $\nu_m = 30\ cm^{-1}$; (---) $S = 0.8$, $\nu_m = 20\ cm^{-1}$; (•••) $S = 0.8$, $\nu_m = 30\ cm^{-1}$; (—••—) $S = 0.5$, $\nu_m = 20\ cm^{-1}$.

In addition to homogeneous broadening, inhomogeneous broadening is also present, due to such factors as statistical fluctuations of the chromophore environment and sample inhomogeneity. This term is generally assumed to be temperature independent and to have a Gaussian distribution (Schomacker & Champion, 1986). At 70K, in the presence of an inhomogeneous contribution of $100\ cm^{-1}$ and using S and ν_m values in the range indicated above, a ratio $FWHM_{high}/FWHM_{low} \leq 1.1$ can be estimated (calculations not shown), thus indicating a small deviation from a purely symmetrical band in the temperature range analyzed. This gives strong physical support to the substantially symmetrical sub-bands obtained by numerical analysis (Zucchelli et al., 1990, 1992, 1994; Jennings et al., 1993; Results) using a decomposition program in which band asymmetry is allowed.

In this respect, a very recent paper (Konermann & Holzwarth, 1996) proposes an asymmetrical shape for the thermally broadened band associated with the 0−0 transition for chls bound to PSII-RC, using coupling factors and mean phonon frequencies obtained by hole burning measurements. In particular, with $S = 0.8$, $\nu_m = 30\ cm^{-1}$, and $FWHM_{inh} \approx 100\ cm^{-1}$, an asymmetric band shape for chl, with a ratio $FWHM_{high}/FWHM_{low} \cong 2$, is suggested at 77 K. This asymmetry remains substantial also at higher temperatures. According to our calculations, these same parameter values yield $\gamma_1 = 0.18$ at 70 K (eq 4), which means a ratio $FWHM_{high}/FWHM_{low} \approx 1.28$ when only the homogeneous contribution at 70 K is considered (Figure 6). This decreases

rapidly with increasing temperature. As stated above, this ratio becames ≤ 1.1 when also the inhomogeneous part (100 cm^{-1}) is taken into account. These calculations are thus in disagreement with the asymmetrical band shape proposed for protein bound chlorophylls.

A thermal analysis of the bandwidth can be performed, in principle, over the entire absorption band, and the result can be directly connected to the properties of the underlying transitions (Appendix). When linear coupling of the electronic transition to vibrational modes is the dominant term in the broadening description of transitions, the mean frequency of the absorption bands does not change with temperature (Lax, 1952) and the second term in eq A.4 or A.5 is a constant. Thus the plot of σ^2 for the entire band versus temperature depends on the $S\nu_m$ values of the underlying transitions. Assuming that all the underlying transitions have similar properties, it is these characteristic $S\nu_m$ values that should be obtained. This analysis (Figure 5) yields $S\nu_m \approx 70$ cm^{-1} while $S\nu_m \approx 16 cm^{-1}$ is the mean value obtained for chl *a* in a protein matrix (Tang et al., 1990; Reddy et al., 1994), a value in approximate agreement with those obtained for the sub-bands analyzed in this paper ($9\ cm^{-1} \leq S\nu_m \leq 14\ cm^{-1}$). It therefore seems that the $S\nu_m$ value obtained from this total absorption analysis is greater than those obtained by hole burning in similar preparations, as well as those obtained for the sub-bands analyzed in this paper, presumably associated with a 20−30 cm^{-1} phonon mode. The next lowest frequency mode reported in the literature for chl *a* in a host protein matrix is around 262 cm^{-1} (Gillie et al., 1989) though it has a very low estimated coupling (0.012) and should not contribute substantially to the thermal broadening of the main band. The greater $S\nu_m$ value obtained from the total absorption strongly indicates that coupling to a low frequency phonon mode is not the only factor responsible for the thermal evolution of band broadening for LHCII. In this context, we have already proposed (Zucchelli et al., 1990, 1994), and confirmed here, that a sub-band which peaks at 684 nm, the intensity of which is strongly temperature sensitive (Figures 1 and 4, Table 1), is present in LHCII. If its contribution, as estimated by numerical decomposition, is subtracted from the absorption band, the thermal analysis yields $S\nu_m \approx 11-20$ cm^{-1}, which is close to the range obtained in the sub-band analysis and in agreement with hole burning data. Thus the "anomalously" high $S\nu_m$ value obtained analyzing the total absorption band can be mainly associated with the presence of sub-bands absorbing at $\lambda \geq 684$ nm having an intensity that depends on temperature. This is strong evidence for the existence of such long wavelength bands in LHCII, a suggestion which has significant implications for energy transfer within LHCII and the PSII antenna.

Temperature-induced changes of the dipole strength of the red-most chl spectral forms affect, in principle, the second term of eqs A.4 and A.5, that is no longer constant. This can formally explain the higher values of the angular coefficient obtained by linear analysis of the entire absorption band. The dipole strength associated with the red-most sub-bands is redistributed to higher energies (Table 1), as the total area remains constant with temperature (not shown). The process responsible for this thermal behavior remains unknown, though an attractive possibility is that the temperature-induced changes in the red-most sub-bands are the effect of coupling of electronic transitions to thermally active vibrational mode(s) with frequencies $\nu_m > 20-30$ cm^{-1}. In this hypothesis, at least part of the sub-bands represent vibronic transitions and the spectral broadening of the absorption band is substantially associated with: (a) coupling to a phonon bath of low frequency ($S_L \approx 0.8-0.5$; $\nu_{mL} \approx 20-30$ cm^{-1}) and (b) a higher frequency mode with mean frequency ν_{mH} and coupling S_H. In this case, the thermal broadening of the absorption band should be described including both frequency contributions (see, e.g., Di Pace et al., 1992):

$$\sigma^2 = S_H \nu_{mH}^2 \coth\left(\frac{h\nu_{mH}}{2k_B T}\right) + 1.39 S_L \nu_{mL} T + \sigma_{inh}^2$$

where the last term is the inhomogeneous contribution. Using this expression to describe the temperature dependence of the entire band (Figure 5), with $S_L\nu_{mL} = 16$ cm^{-1}, as suggested by hole burning (Gillie et al., 1989; Reddy et al., 1994), and $\sigma_{inh} = 266$ cm^{-1}, a frequency mode $\nu_{mH} \approx 120$ cm^{-1} with a coupling $S_H \approx 0.4$ can be roughly estimated.

APPENDIX

For a normalized function $F(x)$ written as a weighted sum of other N functions $f_k(x)$:

$$F(x) = \sum_{k=1}^{N} A_k f_k(x)$$

with

$$\int_{-\infty}^{+\infty} dx\, F(x) = 1; \quad \int_{-\infty}^{+\infty} dx\, f_k(x) = 1; \quad k = 1, ..., N$$

the second central moment, related to the bandwidth σ of $F(x)$, is:

$$\sigma^2 \equiv \int_{-\infty}^{+\infty} dx\, (x - \bar{x})^2 F(x) = \sum_{k=1}^{N} A_k \int_{-\infty}^{+\infty} dx\, (x - \bar{x})^2 f_k(x) \tag{A.1}$$

where $\bar{x}$, the mean value of x as weighted by $F(x)$, is defined as:

$$\bar{x} = \int_{-\infty}^{+\infty} dx\, x\, F(x) = \sum_{k=1}^{N} A_k \int_{-\infty}^{+\infty} dx\, x\, f_k(x) = \sum_{k=1}^{N} A_k \bar{x}_k \tag{A.2}$$

and $\bar{x}_k$ is the mean value of x as weighted by $f_k(x)$. Inserting eq A.2 into eq A.1:

$$\begin{aligned} \sigma^2 &= \int_{-\infty}^{+\infty} dx\, (x - \bar{x})^2 F(x) \\ &= \sum_{k=1}^{N} A_k \int_{-\infty}^{+\infty} dx\, (x - \sum_{r=1}^{N} A_r \bar{x}_r)^2 f_k(x) \end{aligned} \tag{A.3}$$

Obviously,

$$x - \sum_{r=1}^{N} A_r \bar{x}_r = x - \bar{x}_k + \sum_{r=1}^{N} (\bar{x}_k - \bar{x}_r) A_r$$

and then eq A.3 can be written:

$$\sigma^2 = \sum_{k=1}^{N} A_k [\int_{-\infty}^{+\infty} dx\, (x - \bar{x}_k)^2 f_k(x) + (\sum_{r=1}^{N} A_r(\bar{x}_k - \bar{x}_r))^2 \int_{-\infty}^{+\infty} dx\, f_k(x) + 2\sum_{r=1}^{N} A_r(\bar{x}_k - \bar{x}_r) \int_{-\infty}^{+\infty} dx\, (x - \bar{x}_k)\, f_k(x)]$$

$$= \sum_{k=1}^{N} A_k {\sigma_k}^2 + \sum_{k=1}^{N} A_k (\sum_{r=1}^{N} A_r(\bar{x}_k - \bar{x}_r))^2 \qquad (A.4)$$

as the last integral is identically zero. ${\sigma_k}^2$ is the bandwidth of the f_k function ($k = 1, ..., N$).

In the presence of linear coupling between an electronic transition, having dipole strength A_k and a low-frequency vibrational normal mode, only the bandwidth ${\sigma_k}^2$ of the transition band is temperature dependent while $\bar{x}_k$ is a constant (Lax, 1952). In the presence of an inhomogeneous contribution to the bandwidth, it results that

$${\sigma_k}^2 = {\sigma_{k(\mathrm{hom})}}^2(T) + {\sigma_{k(\mathrm{inh})}}^2 = S_k {\nu_{\mathrm{m}k}}^2 \coth\left(\frac{h\nu_{\mathrm{m}k}}{2k_{\mathrm{B}}T}\right) + {\sigma_{k(\mathrm{inh})}}^2$$

and then:

$$\sigma^2 = \sum_{k=1}^{N} A_k S_k {\nu_{\mathrm{m}k}}^2 \coth\left(\frac{h\nu_{\mathrm{m}k}}{2k_{\mathrm{B}}T}\right) + \sum_{k=1}^{N} A_k ({\sigma_{k(\mathrm{inh})}}^2 + (\sum_{r=1}^{N} A_r(\bar{x}_k - \bar{x}_r))^2) \qquad (A.5)$$

From eq A.5 it can be seen that if an absorption spectrum is the sum of different electronic transitions, broadened by coupling to low-frequency normal modes, the σ^2 of the entire band contains two terms; one, not dependent on temperature, associated with the inhomogeneous (statistical) contributions characteristic of the underlying transitions plus contributions due to the presence of these different transitions (heterogeneity), and the other, temperature dependent, which contains the coupling coefficients S_k and the vibrational frequencies $\nu_{\mathrm{m}k}$.

In particular, when all the electronic transitions are coupled to the same bath of low-frequency vibrations, having mean frequency ν_{m} and coupling S, from eq A.5 the bandwidth is given by:

$$\sigma^2 = S{\nu_{\mathrm{m}}}^2 \coth\left(\frac{h\nu_{\mathrm{m}}}{2k_{\mathrm{B}}T}\right) + \mathrm{constant} \approx 1.39 S\nu_{\mathrm{m}} T + \mathrm{constant}; \quad h\nu_{\mathrm{m}} < k_{\mathrm{B}}T \qquad (A.6)$$

REFERENCES

Bevington, P. R., & Robinson, D. K. (1992) *Data Reduction and Error Analysis for the Physical Sciences, 2nd ed.*, McGraw-Hill, New York.

Cattaneo, R., Zucchelli, G., Garlaschi, F. M., Finzi, L., & Jennings R. C. (1995) *Biochemistry 34*, 15267−15275.

Chan, C.-K., & Page, J. B. (1983) *J. Chem. Phys. 79*, 5234−5249.

Dainese, P., & Bassi, R. (1991) *J. Biol. Chem. 266*, 8136−8142.

Dexter, D. L. (1958) in *Solid State Physics. Advances in Research and Applications* (Seitz, F., & Turnbull, D., Eds.) Vol. 6, pp 353−411, Academic Press Publishers, New York.

Di Pace, A., Cupane, A., Leone, M., Vitrano, E., & Cordone, L. (1992) *Biophys. J. 63*, 475−484.

Eadie, W. T., Drijard, D., James, F. E., Roos, M., & Sandoulet, B. (1971) *Statistical Methods in Experimental Physics*, North-Holland Publishing Co., Amsterdam and London.

French, C. S., Brown, J. S., & Lawrence, M. C. (1972) *Plant Physiol. 49*, 421−429.

Gillie, J. K., Small, G. J., & Goldbeck, J. H. (1989) *J. Phys. Chem. 93*, 1620−1627.

Gudowska-Nowak, E., Newton, M. D., & Fajer, J. (1990) *J. Phys. Chem. 94*, 5795−5801.

Gülen, D., & Knox, R. S. (1984) *Photobiochem. Photobiophys. 7*, 277−286.

Hayes, J. M., Gillie, J. K., Tang, D., & Small, G. J. (1988) *Biochim. Biophys. Acta 932*, 287−305.

Hemelrijk, P. W., Kwa, S. L. S., van Grondelle, R., & Dekker, J. P. (1992) *Biochim. Biophys. Acta 1098*, 159−166.

Ide, J. P., Klug, D. R., Kühlbrandt, W., Giorgi, L. B., & Porter, G. (1987) *Biochim. Biophys. Acta 893*, 349−364.

Jennings, R. C., Bassi, R., Garlaschi, F. M., Dainese, P., & Zucchelli, G. (1993) *Biochemistry 32*, 3203−3210.

Jennings, R. C., Zucchelli, G., & Bassi, R. (1996) in *Topics in Current Chemistry: Electron Transfer II* (Mattay, J., Ed.) pp 147−181, Springer, Berlin.

Konermann, L., & Holzwarth, A. R. (1996) *Biochemistry 35*, 829−842.

Krawczyk, S., Krupa, Z., & Maksymiec, W. (1993) *Biochim. Biophys. Acta 1143*, 273−281.

Kühlbrandt, W., & Wang, D. N. (1991) *Nature 350*, 130−134.

Kühlbrandt, W., Wang, D. N., & Fujiyoshi, Y. (1994) *Nature 367*, 614−621.

Kwa, S. L. S.,Groenveld, F. G., Dekker, J. P., van Grondelle, R., van Amerongen, H., Lin, S., & Struve, W. S. (1992) *Biochim. Biophys. Acta 1101*, 143−146.

Kwa, S. L. S., Völker, S., Tilly, N. T., van Grondelle, R., & Dekker, J. P. (1994) *Photochem. Photobiol. 59*, 219−228.

Lax, M. (1952) *J. Chem. Phys. 20*, 1752−1760.

Markham, J. J. (1959) *Rev. Mod. Phys. 31*, 956−989.

Nussberger, S., Dekker, J. P., Kühlbrandt, W., van Bolhuis, B. M., van Grondelle, R., & van Amerongen, H. (1994) *Biochemistry 33*, 14775−14783.

Porra, R. J. (1991) in *Chlorophylls* (Scheer, H., Ed.) pp 31−57, CRC Press, Boca Raton, Ann Arbor, Boston, and London.

Reddy, N. R. S., van Amerongen, H., Kwa, S. L. S., van Grondelle, R., & Small, G. J. (1994) *J. Phys. Chem. 98*, 4729−4735.

Ryrie, I. J., Anderson, J. M., & Goodchild, D. J. (1980) *Eur. J. Biochem. 107*, 345−354.

Schomacker, K. T., & Champion, P. H. (1986) *J. Chem. Phys. 84*, 5314−5325.

Seely, G. R., & Jensen R. G. (1965) *Spectrochim. Acta 21*, 1835−1845.

Stepanov, B. I. (1957) *Sov. Phys. Dokl. 2*, 81−84.

Stepanov, B. I., & Gribkovskii, V. P. (1968) *Theory of Luminescence*, ILIFFE Books Ltd., London.

van Metter, R. L. (1977) *Biochim. Biophys. Acta 462*, 642−658.

van Metter, R. L., & Knox, R. S. (1976) *Chem. Phys. 12*, 333−340.

Zucchelli, G., Jennings, R. C., & Garlaschi, F. M. (1990) *J. Photochem. Photobiol. B: Biol. 6*, 381−394.

Zucchelli, G., Jennings, R. C., & Garlaschi, F. M. (1992) *Biochim. Biophys. Acta 1099*, 163−169.

Zucchelli, G., Dainese, P., Jennings, R. C., Breton, J., Garlaschi, F. M., & Bassi, R. (1994) *Biochemistry 33*, 8982−8990.

BI9613178